ECOGRAPHY

Research

Reduced carbon emissions and fishing pressure are both necessary for equatorial coral reefs to keep up with rising seas

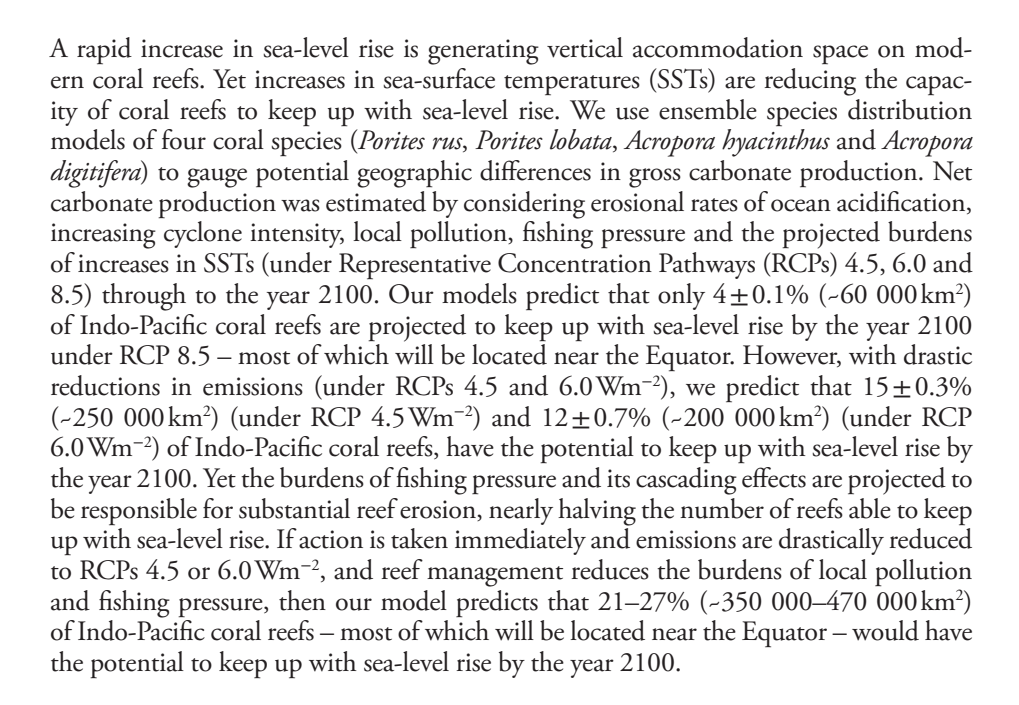
Christopher William Cacciapaglia and Robert van Woesik

C. W. Cacciapaglia (https://orcid.org/0000-0001-8876-3851) (ccacciapagli2008@my.fit.edu) and R. van Woesik, Inst. for Global Ecology, Florida Inst. of Technology, Melbourne, FL, USA.

Ecography 43: 1–12, 2020 doi: 10.1111/ecog.04949

Subject Editor: Julia Baum Editor-in-Chief: Miguel Araújo Accepted 7 February 2020





Keywords: climate change, coral reefs, ecology, modeling

Introduction

After a hiatus of nearly five-thousand years (Lambeck and Chappell 2001), global sea level is rising by an average of 2 mm yr⁻¹ and will most likely increase to 9 mm yr⁻¹ over the next several decades (Vermeer and Rahmstorf 2009, Jevrejeva et al. 2014). Whether coral reefs can keep up with sea-level rise is dependent on the capacity of corals to produce enough calcium carbonate while enduring 1) climate-change induced thermal-stress events (Perry et al. 2013), 2) ocean acidification (Doney et al. 2009), 3) increasing cyclone intensity (IPCC 2013), 4) local pollution (Risk et al. 2009) and



www.ecography.org

© 2020 The Authors. Ecography published by John Wiley & Sons Ltd on behalf of Nordic Society Oikos This is an open access article under the terms of the Creative Commons Attribution License, which permits use, distribution and reproduction in any medium, provided the original work is properly cited.

5) fishing pressure (Carreiro-Silva and McClanahan 2001). Given all of these risks, it is imperative to know where reefs will be most affected by climate-change induced thermal-stress events and other major drivers of change, and to determine whether implementing local management in specific localities, for example by reducing fishing pressure and local pollution, will increase the potential of reefs to keep up with sea-level rise.

The most significant inhibitor of carbonate production on modern reefs is the repeated thermal-stress events that result in coral bleaching and mortality (Loya et al. 2001, Hoegh-Guldberg et al. 2007, Perry et al. 2008). Future carbonate production will depend on the representative concentration pathway (RCP) scenario experienced within the next century, on the intensity and frequency of the resulting thermal-stress events (Perry et al. 2015, van Woesik and Cacciapaglia 2018), and on the spatial distributions and thermal tolerances of major-reef building organisms that have the capacity to build reefs (Fig. 1). In addition, ocean acidification, cyclones, local pollution and fishing pressure also contribute to reef erosion. Ocean acidification

will increase chemical-reef erosion of carbonate framework (Doney et al. 2009). Increasing cyclone intensity and shifts in cyclone trajectories will impact the rates of physical-reef erosion (Gouezo et al. 2015). Increases in human-population densities, local pollution (Risk et al. 2009) and fishing pressure (Carreiro-Silva and McClanahan 2001) will increase biological-reef erosion. We project geographic differences in carbonate production by coral reefs in the Indo-Pacific Ocean while considering the burdens of different climate-change scenarios and the erosional influences of physical, chemical and biological processes through to the year 2100. We consider these pressures on reefs as part of a dynamic system by projecting the potential for increasing thermal stresses under different climate-change scenarios, and projecting changes in cyclone activities, ocean chemistry and human-population densities. These pressures will be evaluated and compared geographically against the capacity of reefs to accrete carbonate structures and keep up with sea-level rise. Reefs that become outpaced by sea-level rise will lose their capacity to protect millions of coastal inhabitants from storm surge and waves.

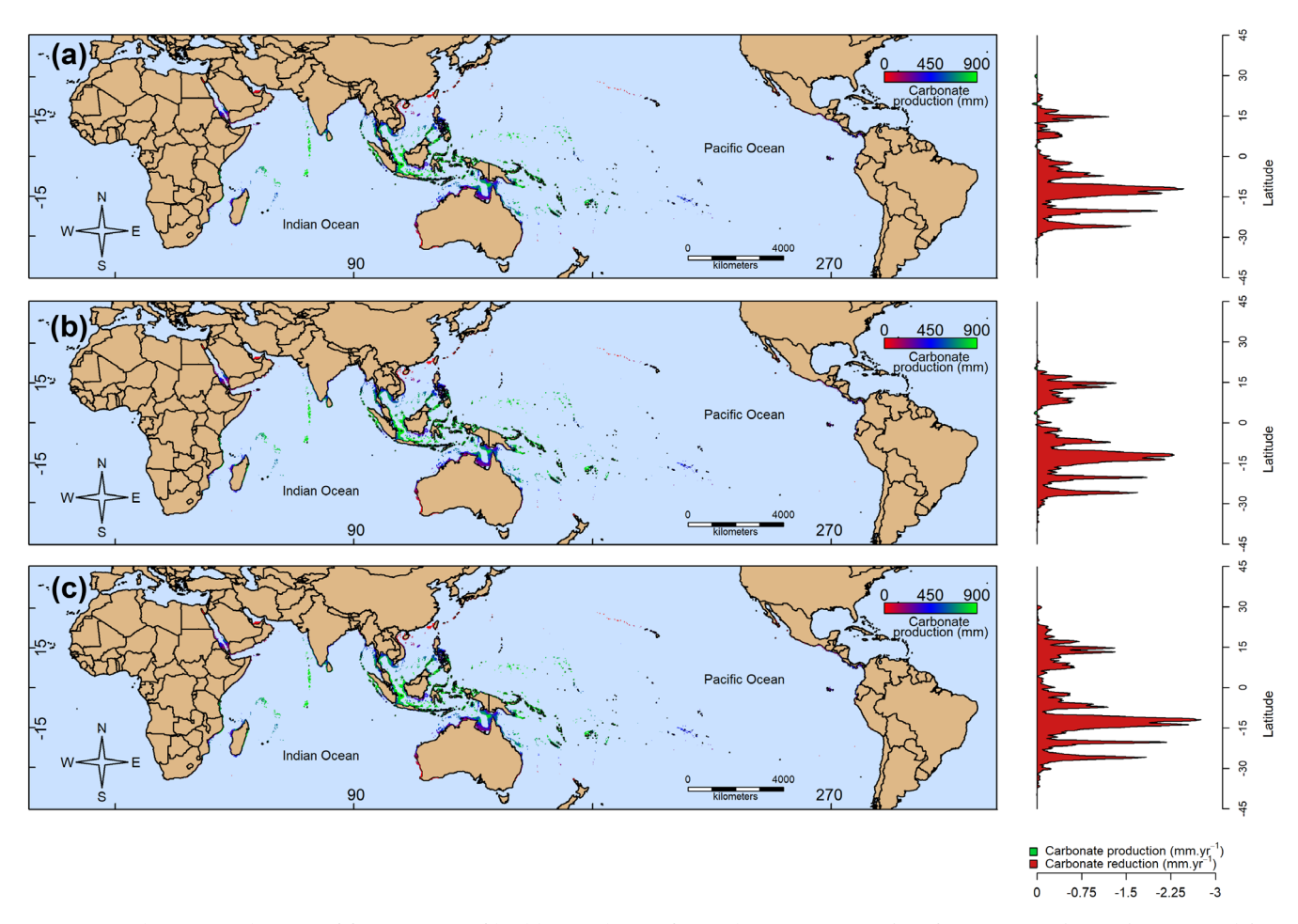


Figure 1. Carbonate production of four major reef-building Indo-Pacific corals (i.e. *Acropora digitifera, Acropora hyacinthus, Porites lobata* and *Porites rus*) under three representative concentration pathways (RCPs) (a) RCP 4.5 Wm⁻², (b) RCP 6.0 Wm⁻² and (c) RCP 8.5 Wm⁻² through to the year 2100. Side plots indicate the change in rate of carbonate production between contemporary model runs and model runs in 2094 as ten-year averaged time periods.

Material and methods

Species distribution model

We first sought to determine where in the Indian and Pacific Oceans corals might be able to grow and build reefs into the near future given different greenhouse gas emission scenarios. We selected four major Indo-Pacific reef-building coral species, Acropora digitifera, Acropora hyacinthus, Porites lobata and Porites rus. These species were chosen to represent the general response of reef-building corals to sea-level rise because of their ubiquity in the Indo-Pacific and because of their variation in susceptibility to thermal stress. Porites lobata and P. rus are generally more tolerant to thermal stress than Acropora species (Loya et al. 2001). To rationalize our approach of selecting four coral species, instead of modeling all of the hundreds of extant coral species, we point to recent studies in Micronesia that found that over 80% of carbonate production of a given reef was contributed by as few as five coral species (van Woesik and Cacciapaglia 2019), and in general less than 10% of the coral species contributed upwards of 75% of the reef's carbonate production (van Woesik and Cacciapaglia 2018). Furthermore, although dominant coral species differ across reefs, there is considerable functional redundancy in terms of carbonate production, with different dominant species producing similar rates of carbonate production (van Woesik and Cacciapaglia 2018, 2019). We note that other coral species can be added to the model, although here we use four coral species as a proof-of-concept.

The geographic localities of the four coral species were recorded as either present or absent, with > 95% certainty, using a probability-of-detection algorithm (Cacciapaglia and van Woesik 2015). The geographical distribution of the

coral species were determined using Veron (2000), IUCN's Red List <www.iucnredlist.org/technical-documents/spatialdata>, and Wallace (1999). We used a generalized-linear mixed model in a Bayesian framework to examine the relationship between the species likelihood of occurrence and the following environmental covariates: 1) range in sea surface temperature (SST), 2) range in irradiance and 3) turbidity. The environmental layers were derived from Cacciapaglia and van Woesik (2016). Sea-surface temperature (SST) data were gathered from Bio-ORACLE (Ocean Rasters for Analysis of Climate and Environment) (<www.oracle.ugent. be/>), which were derived from Aqua-MODIS (Moderate Resolution Imaging Spectroradiometer) satellite for the years 2002-2009 (Tyberghein et al. 2012). The data were adjusted to grids of 5 arc minutes (ca 9.2 km) using bilinear interpolation. Irradiance was assessed as Photosynthetically Available Radiation (PAR, μEm⁻²s⁻¹) using the satellite Sea-Viewing Wide Field-of-View Sensor (SeaWiFS) (http://gdata1. sci.gsfc.nasa.gov/daac-bin/G3/gui.cgi?instance id=ocean month>) at a resolution of 9 × 9 km². Turbidity was assessed as the diffuse attenuation coefficient of the downwelling spectral irradiance wavelength 490 nm (K_d 490), also using SeaWiFS (Pierson et al. 2008). Environmental conditions at grid cells of 9.2 km (outlined below) were extracted at 3000 points, chosen to cover the geographic extent where the species was present and absent. Turbidity was expressed as a random effect, binned to remove no-analog scenarios. The bin size for turbidity was optimized to reduce the model's Akaike's information criterion score. An ensemble of twenty-five model runs, each selecting the highest area under the receiving operating curve using 100 random iterations (Cacciapaglia and van Woesik 2015), were run to predict modern and future distributions for each of the four coral species.

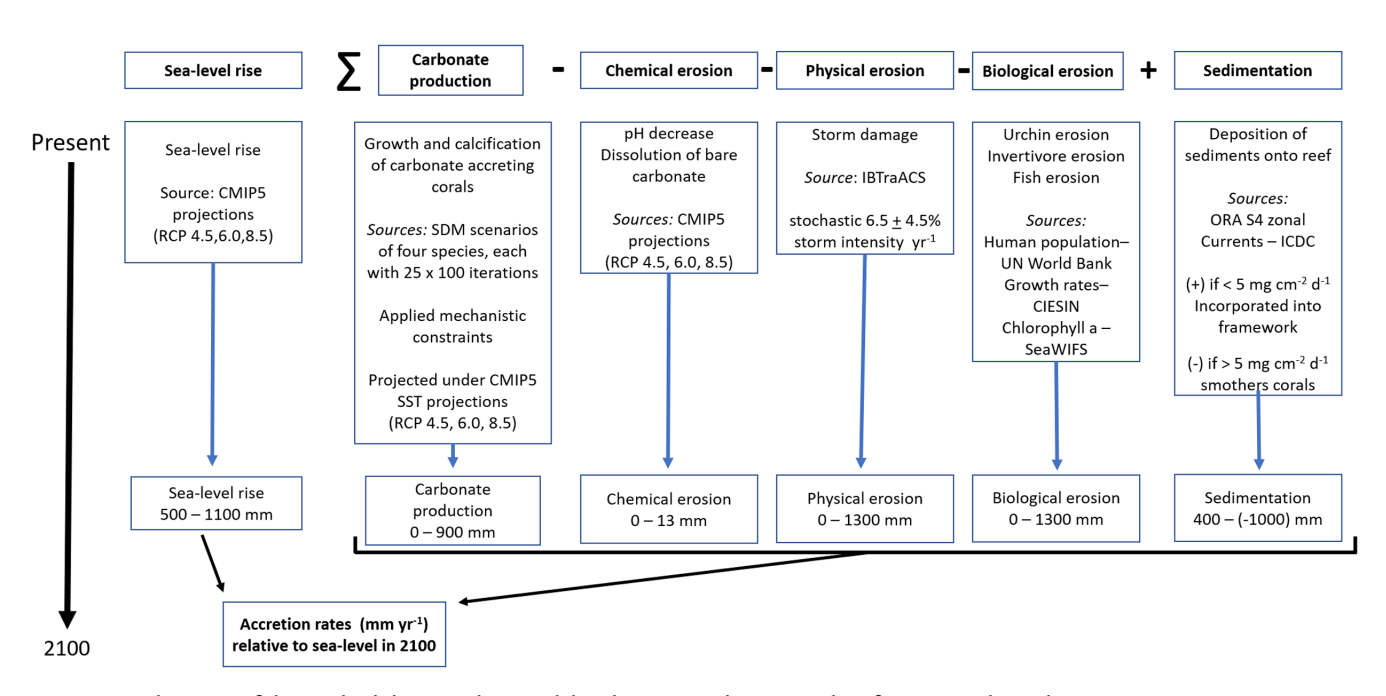


Figure 2. A schematic of the methodology used to model carbonate production and reef accretion through time.

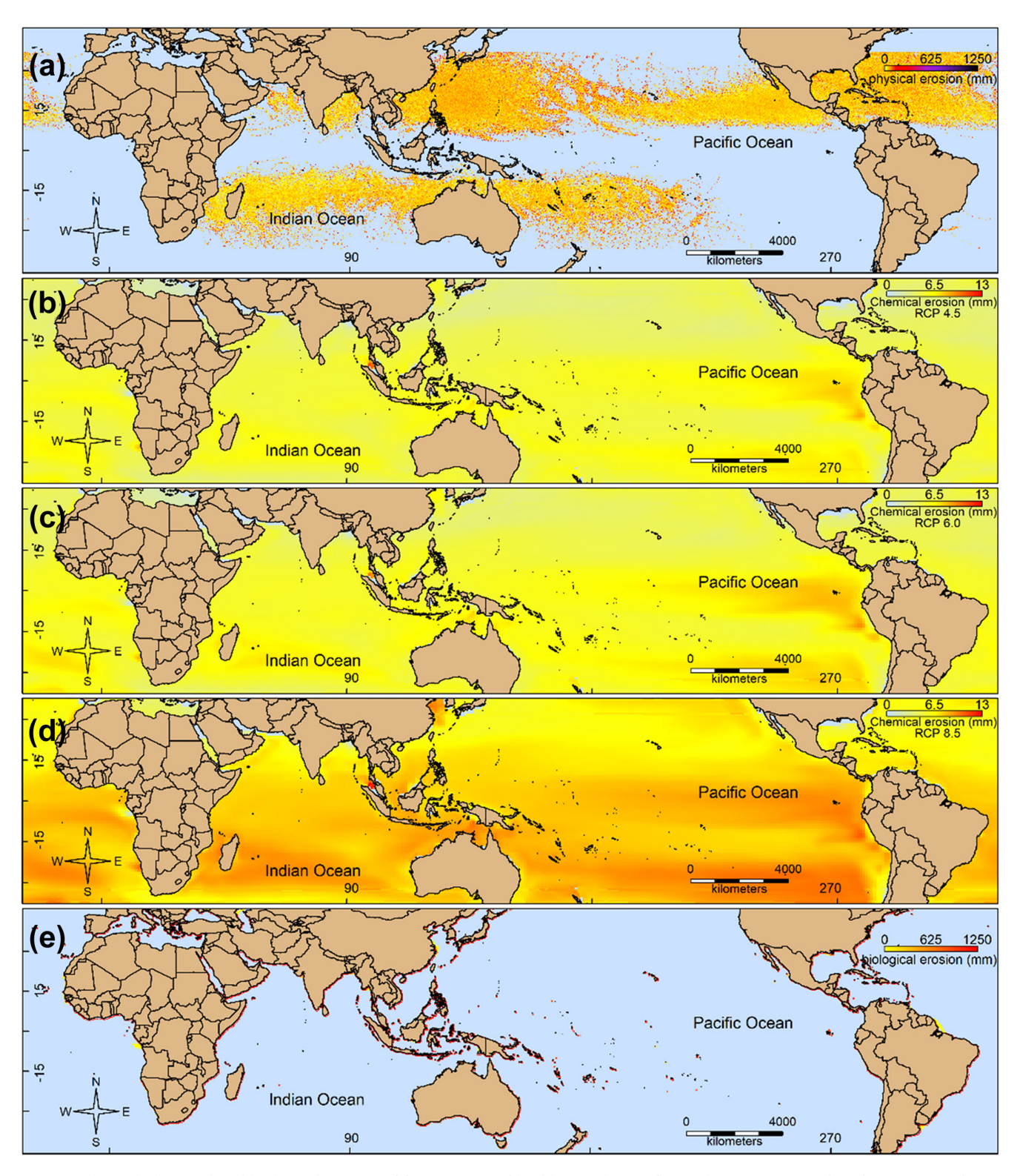


Figure 3. Physical, chemical and biological erosion of four major reef-building Indo-Pacific corals (i.e. *Acropora digitifera*, *Acropora hyacinthus*, *Porites lobata* and *Porites rus*) under three different representative concentration pathways (RCPs) through to the year 2100. (a) Physical erosion (mm) caused by cyclones, (b) chemical erosion (mm) from ocean acidification under RCP 4.5 Wm⁻², (c) chemical erosion (mm) from ocean acidification under RCP 8.5 Wm⁻² and (e) biological erosion (mm) caused by sea urchins and parrotfishes, and infaunal organisms, such as boring sponges, polychaetes and sipunculids.

Mechanistic constraints

Mechanistic constraints were applied to the output of each species distribution model, to realistically constrain model estimates without increasing model complexity. These mechanistic constraints were based on Cacciapaglia and van Woesik (2015) and were implemented as follows. First, a dispersal restriction was implemented to limit the distance of annual range expansion to 10 km yr⁻¹ based on reproductive studies (Miller and Mundy 2003, Shanks et al. 2003, van Woesik 2010), dispersal models incorporating warming oceans (O'Connor et al. 2007, Figueiredo et al. 2014), and genetic studies (Ayre and Hughes 2000). Second, the outflow areas of large rivers, where freshwater jeopardizes coral survival, were masked out as viable habitats based on drainage size. Third, a cold-water mask was implemented, excluding all reef habitats that experience < 18°C at any time of the year (Kleypas 1997, Kleypas et al. 1999). Fourth, a mask was applied outside of the contiguous oceanic region, where species experience geographic isolation. Fifth, any site that experienced $< 250 \,\mu \text{mol}\,\text{m}^{-2}\,\text{s}^{-1}$ irradiance at 3 m depth was masked out as the water was considered too turbid for adequate photosynthesis and reef growth (Kleypas et al. 1999). The difference between modern-day species distributions and future species distributions was interpolated linearly through time so that we could estimate intermediate probabilities of species presence, at each time step of the model (all R code for the model and the Google Earth kmz files are available in Supplementary material Appendix 1 and at https://github. com/InstituteForGlobalEcology>). Each model was run for 100 iterations to gain confidence in the projected estimates.

Carbonate production model

In its simplest form, carbonate production (kg CaCO₃ m⁻²) was modeled at a given locality i, with a spatial resolution of 5-arc minutes (or 9.2 km cell size) at a given time, t, as:

Carbonate production_{i,t} =
$$Cal_{i,t} + sgn(x)Sed_{i,t} - Eros_{i,t}$$
 (1)

where Cal is the rate of calcification by reef-building corals and other calcareous organisms, sgn influences sedimentation (Sed) and acts as a switch from positive (+) to negative (–), based on research from van Woesik (2013) stemming from regional studies around the world, where sedimentation $<5\,\mathrm{mg\,cm^{-2}\,d^{-1}}$ causes a positive (+) increase in carbonate

production, but > 5 mg cm⁻² d⁻¹ (after Rogers 1990) causes a net decrease (–) of carbonate productivity, because the sediment smothers reefs and is a deterrent to positive carbonate production. Although Rogers (1990) specified a threshold of $10 \, \text{mg cm}^{-2} \, \text{d}^{-1}$, we sought to be more conservative in our estimates. Eros is the rate of erosion (van Woesik 2013). t is the time step of five years up until the year 2100 (Fig. 2).

Calcification was assumed to follow optimal performance curves, or niche space, taking the form of Gaussian distributions, dependent on sea surface temperature (SST) and irradiance (Supplementary material Appendix 1 Fig. A9). The SST component of the model varied through time, assessed at 5-yr intervals based on representative concentration pathway (RCP) 8.5 Wm⁻² model scenarios from the Coupled Model Intercomparison Project Phase 5 (CMIP5) (Cacciapaglia and van Woesik 2015). Optimal values for SST and irradiance were derived from the respective median and mean values of current environmental data extracted at the presence points where the four coral species were located.

Maximum calcium carbonate production under modern-day climate is approximately 12 kg CaCO₃ m⁻² (Edinger et al. 2000), although higher values have been reported (Perry et al. 2018, van Woesik and Cacciapaglia 2018). For the purpose of this model, however, given the spatial resolution of 9.2 km, we assumed that carbonate production was most optimal, in a given locality, i, in the presence of all four species. We therefore allocated a maximum reef-building capacity of 3 kg CaCO₃ m⁻² yr⁻¹ for each of the four coral species, and the capacity to occupy space made available by the removal of other species by projected thermal stress. The rationale was to examine where, geographically, all four coral species might maintain their reefbuilding capacity and contribute to carbonate production as a general response of reef-building corals to sea-level rise and thermal stress. To account for the allometric reduction in reef height as calcium carbonate increases, mass carbonate production (kg CaCO₃ m⁻² yr⁻¹) was translated to vertical reef growth (mm yr⁻¹) using:

Vertical reef growth =
$$Cp + Cp(Cp \times alpha)$$
 (2)

where Cp is carbonate production and alpha is an estimated coefficient (0.0002 in this model) where kg is the amount of 2-dimensional carbonate production per year ($kg CaCO_3 m^{-2}$).

Table 1. Summary of physical, chemical and biological annual-erosion rates of four major reef-building Indo-Pacific corals (i.e. *Acropora digitifera, A. hyacinthus, Porites lobata* and *P. rus*), and the influence on the rates of vertical coral reef accretion through to the year 2100 under three representative concentration pathways (RCPs) 4.5, 6.0 and 8.5 Wm⁻².

RCP (Wm ⁻²)	Carbonate production (mm yr ⁻¹)	Physical erosion (mm yr ⁻¹)	Chemical erosion (mm yr ⁻¹)	Biological erosion (mm yr ⁻¹)	Sea-level rise (mm yr ⁻¹)	Net reef accretion (mm yr ⁻¹)	Carbonate production rate (mm yr ⁻¹)
RCP 4.5	6.21 ± 0.45	0.67 ± 0.01	0.057	9.4	6.30	-10.5 ± 0.08	-0.12 ± 0.05
RCP 6.0	6.16 ± 0.49	0.67 ± 0.01	0.062	9.4	6.76	-11.1 ± 0.09	-0.14 ± 0.05
RCP 8.5	6.42 ± 0.22	0.67 ± 0.01	0.088	9.4	8.66	-12.9 ± 0.02	-0.17 ± 0.01

Habitat availability

Climate change can cause the loss of susceptible coral species from reefs and the gain of more thermally tolerant species (Loya et al. 2001). Such species shifts and compensatory adjustments were considered in the current predictions. The available space that could be taken over by an opportunistic, thermally tolerant species was dependent on the local prevalence of the opportunistic species under future climate scenarios. The capability of each coral species to occupy newly available space was calculated as followed:

$$SprevF_i = Sprev_i + Sprev_i / 25 \times dif_i / 3 \times efficiency$$
 (3)

where $\operatorname{Sprev} F_i$ is the future prevalence of a species i, Sprev_i , is the modeled prevalence of species i, dif is the available habitat space provided by the reduction of species j. Twenty-five is a constant, used to convert model runs into prevalence, three is the number of species capable of occupying newly available space. The parameter efficiency was set at 0.5 to allow tolerant species to recover up to half of the habitat that was made available by losing susceptible species. This parameter was added to account for competition among other organisms, such as macroalgae, competing for available space. Before species j could occupy the space of species j, the mechanistic constraints on habitat availability included: 1) that the prevalence of species j had to decrease below 50% occupancy, under pressure from climate change, and 2) for a species j to take over the space, it had to have a local prevalence j 50% occupancy.

Sedimentation

Sedimentation (mg cm⁻² d⁻¹) was estimated using the inverse logarithm of average water-flow rate (ms⁻¹) data, which were collected from the Integrated Climate Data Center (ICDC; http://icdc.zmaw.de/). The zonal and meridional velocities of water flow, at 5 m depth, were averaged from 2006 to 2010, and Pythagoras's theorem was used to find directionless flow rate per locality (at a spatial resolution of 9.2 km). This estimated flow rate was used as a proxy for sedimentation, which was previously validated with in-situ data collected by sedimentation traps by Rogers (1990) and Szmytkiewicz and Zalewska (2014). For the purposes of the model, flow rate was assumed to remain constant between the years 2010 and 2100. Again, if the rate of sedimentation was between 0 and 5 mg cm⁻² d⁻¹ then the sign of sedimentation, in Eq. 1, was positive, if sedimentation was greater than 5 mg cm⁻² d⁻¹ then the sign was negative (van Woesik 2013; based on regional studies from the Caribbean, Hawaii and the Atlantic Ocean).

The maximum reduction of calcification rates caused by sedimentation was adjusted to match the total growth of the reef in each 9.2 km cell, so that the effect of sedimentation, in this model, could inhibit reef growth, but would not cause erosion. We also factored in that about two thirds of the sediments were exported from the reef (Hubbard 1986).

Erosion

Reef erosion was broken down into three major components, defined as:

$$Eros_{i,t} = phy.erosion_{i,t} + chem.erosion_{i,t} + bio.erosion_{i,t}$$
 (4)

where phy.erosion is the physical erosion caused by cyclones, chm.erosion is the chemical dissolution of reef caused by ocean acidification, and bio.erosion is the biological erosion caused by marine organisms. To determine physical erosion, cyclone data were collected from International Best Track Archive for Climate Stewardship (IBTrACS; <www.ncdc.noaa.gov/ibtracs/index.php?name=ibtracsdata>) as spatial points and imported into R (R Core Team, ver. 3.22). These data were subset into storm categories based on wind speed, according to the Saffir-Simpson scale. A raster file for the spatial frequency of cyclones was made in Quantum Geographical Information Systems (QGIS) using the 'heatmap' function, with a radius matching the radius of damaging winds (> 26 ms⁻¹) for each cyclone category (Supplementary material Appendix 1). These radii followed Moyer et al. (2007) and considered 50 yr of consistent sampling effort, between 1964 and 2014. Individual yearly raster files were summed, and then divided by 50 yr to determine the average number of cyclones per 9.2 km cell yr⁻¹. A raster for the magnitude of the cyclones was created by interpolating wind speeds across all storm tracks using the inverse distance weighted interpolation in QGIS. For the model, the maximum amount of CaCO3 that any given cyclone could remove was set to 1350 kg m⁻² for the modern-day intensity. This 1350 kg CaCO₃ m⁻² removal matches approximately 1 m of vertical reef growth, which has been observed after large cyclones pass over reefs that infrequently experience cyclones (van Woesik et al. 1991). We matched the highest rates of physical erosion with localities that experienced few cyclones in the past. The increasing intensity of storms predicted by 2100 of 2-11% (Knutson et al. 2010) was incorporated by stochastically sampling from a normal distribution of $6.5 \pm 4.5\%$ that increased linearly from no effect in contemporary model runs to the full 6.5% increase by 2100 (Supplementary material Appendix 1 Fig. A10). Storm

Table 2. Percentage of Indo-Pacific coral reefs that will keep up with sea-level rise through to the year 2100 with, and without, reductions in fishing pressure under three representative concentration pathways (RCPs) 4.5, 6.0 and 8.5 Wm⁻².

RCP (Wm ⁻²)	Projected % of reefs keeping up with sea-level rise, with fishing pressure	Projected % of reefs keeping up with sea-level rise, without fishing pressure
RCP 4.5	$15.0 \pm 0.31\%$	$27.3 \pm 0.7\%$
RCP 6.0	$12.3 \pm 0.69\%$	$21.0 \pm 1.1\%$
RCP 8.5	$3.7 \pm 0.13\%$	$4.6 \pm 0.2\%$

frequency was represented as a binomial distribution using the following equation:

Storm frequency =
$$\binom{T \times 365}{k} \left(\frac{p}{365}\right)^k \left(1 - \frac{p}{365}\right)^{T \times 365 - k}$$
 (5)

where k is the estimated number of cyclones over time T (years), and p is the average number of storms observed per year, per raster cell. The estimated number of cyclones over the projected time was then multiplied by the potential storm damage in each raster cell, i (Fig. 3a).

Chemical erosion

Chemical erosion was incorporated into the model by using pH as the measure for ocean acidification. The CMIP5 projected pH data, for the global climate model of RCP 8.5 Wm⁻², RCP 6.0 Wm⁻² and RCP 4.5 Wm⁻² were collected as global raster images for the years 2006–2100 from <ftp://data1.gfdl.noaa.gov/11/CMIP5/output1/NOAA-GFDL/GFDL-ESM2M/> as a 1×1 degree raster. These raster data were collected at 5-year-averaged intervals and transformed to match the environmental parameters used in the species distribution model. A linear model, using data from van Woesik et al. (2013) was run to determine how much calcium carbonate is potentially lost, based on pH. This relationship follows the following equation:

Chm.erosion =
$$(6.65 - 0.81x)^{1.667}$$
 (6)

where chm.erosion is the reduction in carbonate measured as kg CaCO $_3$ m $^{-2}$ yr $^{-1}$. The level of chemical erosion was predicted in each 9.2 km cell of the raster, based on the ocean surface pH at each 5-yr time interval. The sum of predicted erosion, for all time steps between 2006 and 2100, was calculated in each 9.2 km raster cell and summed to determine the overall potential loss of CaCO $_3$. Chemical erosion was modeled as an effect of calcium carbonate dissolution, and not as an effect of reef-growth inhibition because of the ability of corals to internally regulate pH (McCulloch et al. 2012).

Biological erosion – external

Biological erosion was broken down into two primary components: 1) bioerosion from sea urchins and parrotfishes, and 2) bioerosion from infaunal organisms, such as boring sponges, polychaetes and sipunculids. Silva and McClanahan (2001) showed that maximum bioerosion was inversely related to the densities of invertivore-fish populations. Williams et al. (2011) showed that the loss of densities of invertivore fishes and fishing pressure were positively related to human population densities following the function:

$$Biomass = -2.73 \times log10(population + 1) + 17.23 \tag{7}$$

where biomass is the biomass of secondary-trophic level fishes, and population is the human population summed within a 30 km radius of each grid cell. We calculated human population densities, using human densities from the Center

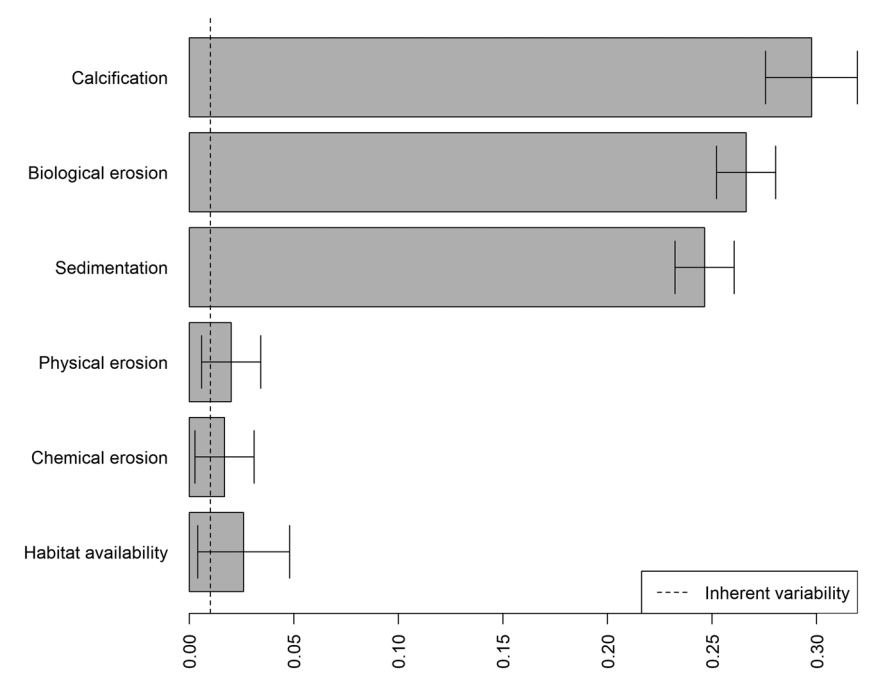


Figure 4. Sensitivity plot of six key variables involved in carbonate production. The models were re-run by adding and subtracting 10% of the production rates (kg CaCO $_3$ m 2 yr $^{-1}$) from each of the variables. The graphs show the contribution of each variable as a proportion to net carbonate accretion (mm) in the year 2100 under climate scenario RCP 8.5. Habitat availability was determined by taking 10% of the difference in net carbonate production between model runs that included and didn't include habitat availability. The inherent variability (dotted line) conveys the extent of stochasticity of the species distribution models.

for International Earth Science Information Network, which were then aggregated to the $9\times9\,\mathrm{km}$ grid cells and summed within a 30 km radius of each grid cell to match the coastal population densities. Thirty kilometers was considered optimal after testing various buffer sizes to match the coastal

populations (following Williams et al. 2011). Human population was projected into the year 2100 using birth and death rates aggregated for each country (collected from the World Bank as the adjusted UN census for 2015), and the difference between birth and death represented growth rate. A carrying

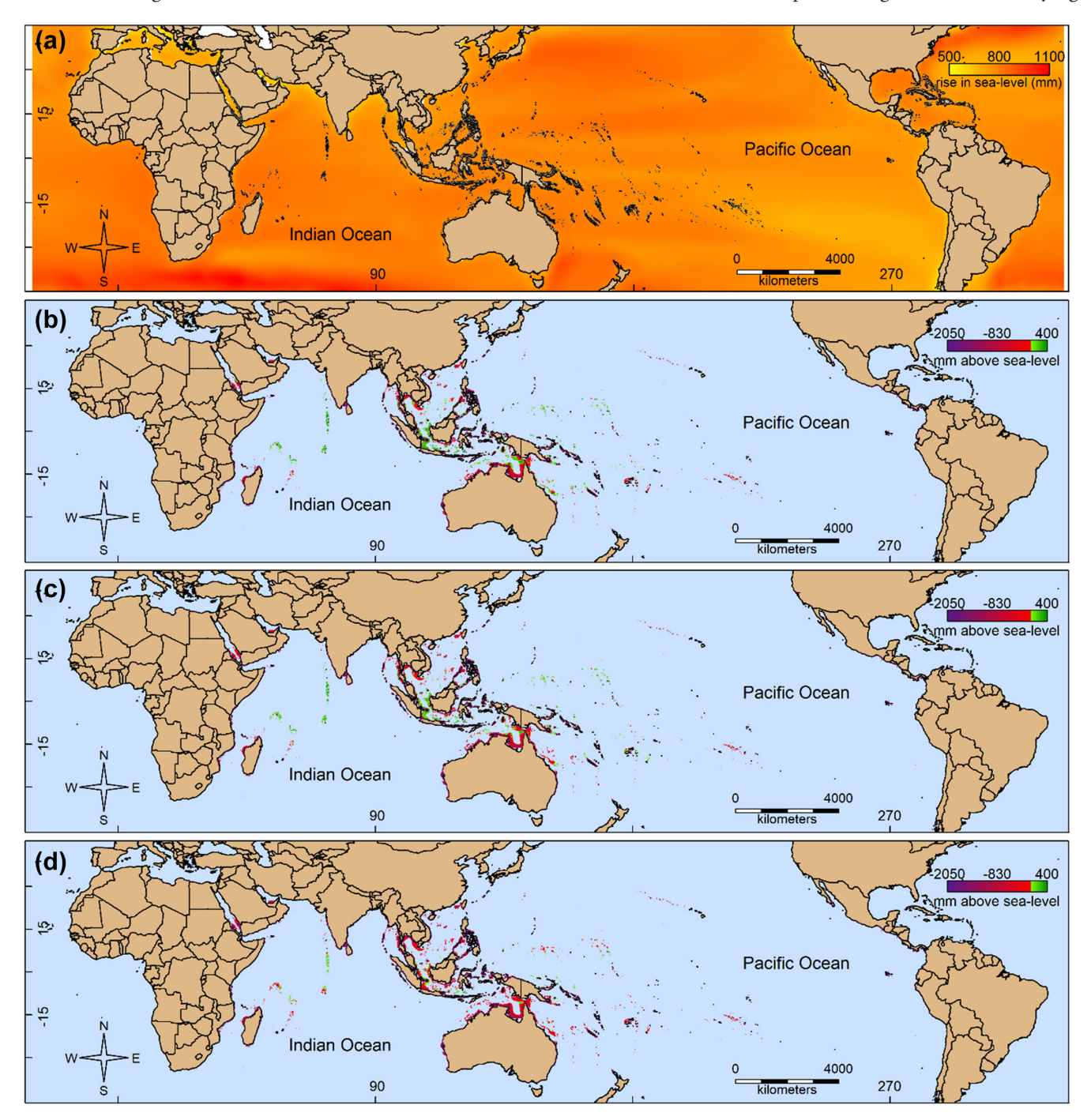


Figure 5. The predicted sea-level rise and the projected distribution and height (mm) above sea level of four primary Indo-Pacific reef-building corals (i.e. *Acropora digitifera*, *Acropora hyacinthus*, *Porites lobata* and *Porites rus*) under three different representative concentration pathways (RCPs) through to the year 2100. (a) The predicted rise in sea level by 2100 under RCP 8.5 Wm⁻². (b) The projected future reef height under RCP 4.5 Wm⁻². (c) The projected future reef height under RCP 8.5 Wm⁻². Where red to purple indicates the geographic location of 'sinking' reefs, and light green to dark green indicates reefs that were predicted to be able to 'keep up' with sea-level rise.

capacity of 11.2 billion was used, matching estimates from the United Nations (current 2019 estimates have a 95% confidence interval of \pm 1.8 billion people). Population growth rates were attached to shapefiles and converted to raster data. A moving-window analysis was applied to each time-step raster (using the 'focal' function from the package 'raster' [Hijmans et al. 2014]), to match the 30 km buffer size and the resulting aggregated-human-population raster was used in Eq. 7 to then estimate invertivore fishes and the resulting sea-urchin densities as shown in Eq. 8. Human coastal populations were reassessed at each 5-yr time step, and erosion was summed throughout the model run. The maximum rate of erosion by urchins was found to be 22.3 kg m⁻² yr⁻¹, following relationships and data from McClanahan and Shafir (1990) and Silva and McClanahan (2001) (where invertivore-fish population densities were minimal), using:

Urchin eros =
$$(\text{Biomass} \times -1 + 30)/1.32$$
 (8)

where Urchin_eros is the erosion by sea urchins following the Biomass of secondary-trophic level fishes. Herbivorous parrotfish erosion was estimated using a regression from estimated densities of urchins and parrotfish following Eq. 9 derived from studies in Micronesia (van Woesik and Cacciapaglia 2018) and in the Caribbean (Perry et al. 2013):

$$Fish_eros = exp(-8.0025 \times Urchin_eros + 0.8190)$$
 (9)

where Fish_eros is the herbivorous parrotfish erosion following the Urchin_eros found in Eq. 8.

Biological erosion – internal

Eutrophic areas often have high levels of internal bioerosion (Hallock and Schlager 1986, Edinger and Risk 1994). In this model, locations that had high and persistent concentrations of chlorophyll *a*, were considered eutrophic. We used time-averaged chlorophyll *a* as a proxy for infaunal bioerosion. Chlorophyll *a* data were collected from SeaWIFS satellite observations, and time averaged from 1998 to 2007. These data were cropped between the latitudes 45°S and 45°N and used as a proxy for internal bioerosion of micro- and macroboring organisms. The maximum rate of internal erosion, 2.4 kg m⁻² yr⁻¹ which was estimated by Pari et al. (1998), was used to scale the chlorophyll raster into a proxy for internal erosion. In this model, internal bioerosion is assumed to remain constant into the future.

Sea-level rise

Sea-level rise data were extracted from the Integrated Climate Data Center (ICDC) as the representative concentration pathway (RCP) 8.5 Wm⁻² and RCP 4.5 Wm⁻² ensemble mean. These data were extracted at yearly intervals so that the model could be run for each year leading up to 2100. RCP 6.0 Wm⁻² data were only available for the year 2100 from ICDC and were therefore extrapolated at yearly intervals with the assumption that RCP 6.0 follows a similar spatial relationship to RCP 8.5 and RCP 4.5 in 2100 as it does through all other years. The rate of sea-level rise was compared with rates of vertical reef growth at a spatial resolution of 9.2 km through to the year 2100.

Results and discussion

Increasing thermal stress associated with higher RCP scenarios showed considerable shifts in coral-species distributions in the Indo-Pacific Ocean through to the year 2100 (Supplementary material Appendix 1 Fig. A1). These species shifts caused major reductions in carbonate production in some geographic regions, particularly on reefs between the latitudes $10-15^{\circ}$ south, under an $8.5\,\mathrm{Wm^{-2}}$ RCP scenario (Fig. 1, Supplementary material Appendix 1 Fig. A2). The smallest losses of carbonate production were predicted just north of the Equator in Indonesia (Fig. 1), and the largest losses coincided with the highest thermal anomalies between the latitudes of $10-20^{\circ}$ in both the northern and southern hemispheres (Supplementary material Appendix 1 Fig. A3, A4).

Our predictions estimated that cyclones are locally capable of causing the largest reductions in carbonate production, particularly in localities that have historically experienced low cyclone activity. The greatest cyclone impact is predicted to occur between latitudes 5° and 15° north, near the periphery of observed present-day cyclone tracks (Fig. 3a, Supplementary material Appendix 1 Fig. A5). Although capable of significant local destruction, cyclones are not predicted to be the main suppressor of future reef growth, because they are geographically focused events (Fig. 3a). Chemical erosion, in the form of ocean acidification, also had a relatively low predicted impact on carbonate production (Table 1), at least compared with other variables that were considered in the current model. Under the projections for this model, ocean acidification is predicted to reduce vertical reef growth of Indo-Pacific corals by 0.08, 0.06 and 0.05 mm yr⁻¹ under RCPs 8.5, 6.0 and 4.5 Wm⁻² respectively (Table 1). Areas most likely to experience the highest chemical-erosion rates

Table 3. Predicted areas of Indo-Pacific coral reefs that will keep up with sea-level rise through to the year 2100 (years 2086–2094) under three representative concentration pathways (RCPs) 4.5, 6.0 and 8.5 Wm⁻².

RCP (Wm ⁻²)	Area of coral reef at sea-level (km²)	Area of drowned reef (km²)	Percentage of coral reef able to keep up with sea-level rise until 2100
RCP 4.5	$250\ 000 \pm 5000$	$1\ 400\ 000 \pm 5000$	15.0 ± 0.31
RCP 6.0	$200\ 000 \pm 11\ 000$	$1\ 440\ 000 \pm 11\ 000$	12.3 ± 0.69
RCP 8.5	$60\ 000 \pm 2000$	1580000 ± 2000	3.7 ± 0.13

were in northern Malaysia, western Japan and along the northwestern coast of Australia (Fig. 3b-d).

Compared with physical- and chemical-erosion rates, biological erosion was predicted to have the highest impact on future carbonate production (Table 2). Our predictive models estimated that coral reefs impacted by fishing pressure appear most vulnerable. The projected increase in human population density to 11.2 billion people by the year 2100, is likely to result in the further removal of large carnivorous fishes from reefs, which Carreiro-Silva and McClanahan (2001) showed would increase the density of herbivorous invertebrates and increase erosion rates. In the absence of fishing pressure, the number of reefs capable of keeping up with sea-level rise was predicted to drastically increase, especially under reduced greenhouse emissions. Under RCP 4.5 Wm⁻², a lack of fishing pressure was predicted to allow 82±9.8% more Indo-Pacific coral reefs (-230 000 km²) to keep up with sea-level rise, and those under RCP $6.0\,\mathrm{Wm^{-2}}$ were predicted to have a $71\pm16\%$ increase (~150 000 km²), whereas estimates under a RCP 8.5 Wm⁻² scenario were predicted to have a 24±23% increase (~16 000 km²) (Table 2, Supplementary material Appendix 1 Fig. A6). The highest biological-erosion rates were predicted to occur on the coral reefs in India, China, sub-Saharan Africa, Madagascar, Central America, and in densely populated regions of Indonesia (Fig. 3e). There is however considerable uncertainty associated with the projected rates of biological erosion. Although we used high resolution data for contemporary human population densities (9 km grid size), the available population growth rates were aggregated by country. Given the assumptions and sensitivities (Fig. 4) associated with biological erosion in the projections of carbonate production, it seems that regional and local studies are needed to improve the model projections and reduce the uncertainties associated with biological erosion.

If greenhouse gas emissions are drastically reduced by 2100 (under RCP 4.5 Wm⁻²), but Indo-Pacific coral reefs are still subjected to the burdens of increasing cyclone intensity, ocean acidification, local pollution and fishing pressure, then only $15 \pm 0.3\%$ (250 000 km²) of coral reefs are predicted to produce enough carbonate to keep up with sea-level rise (Fig. 5b, Supplementary material Appendix 1 Fig. A6). However, if coral reefs are subject to the same burdens until 2100 under RCPs 6.0 and 8.5 $\mathrm{Wm^{-2}}$, $12 \pm 0.7\%$ (200 000 km²) and $4 \pm 0.1\%$ (60 000 km²) of coral reefs, respectively, are projected to keep up with sea-level rise (Fig. 5c-d) – most of which were estimated to be located near the Equator (Fig. 5). High latitude coral reefs are more likely to drown because of high erosion rates relative to production rates (Fig. 1, 2, Supplementary material Appendix 1 Fig. A2, A7), which are exacerbated by limited irradiance at high latitudes (Muir et al. 2015). These model estimates agree with recent field studies on coral bleaching, which show lower probabilities of coral bleaching near the Equator than elsewhere (Sully et al. 2019). In agreement with these models and recent field estimates, Penn et al. (2018) showed that in a simulated mass extinction event of the Permian-Triassic boundary, with an increase in SST of 10°C, species near the Equator were more likely to persist than their counterparts at

higher latitudes, mainly because equatorial species were already adapted to warmer conditions.

There are however several caveats that should be considered when interpreting the outputs of the current models. Firstly, although we used dominant reef-building corals, there are unaccounted uncertainties when using proxies and substituting four coral species for a reef assemblage. Sensitivity analyses showed that indeed changes in carbonate production, caused by shifts in the composition and abundance of calcareous organisms, were the most sensitive aspects of the current model (Fig. 4). Future models may seek to include other coral species and other calcareous organisms (see R code in Supplementary material Appendix 1). Changes in urchin and fish densities and sedimentation rates were also sensitive parameters of the model (Fig. 4), suggesting that human population densities, fishing pressure and land-use changes have considerable influences over whether a coral reef can keep up with sea-level rise. Our models were less sensitive to physical and chemical erosion and habitat availability. Yet, there are also unknown interactions and interdependencies with neighboring habitats and ecosystems that were not incorporated in the current model, such as the presence of sea grasses (Manzello et al. 2012, Sanders et al. 2014), which may influence carbonate production of adjacent coral reefs. There is also a need to refine parameters, such as the efficiency coefficient in habitat availability (Eq. 3). Although refining some of these uncertainties, as more data become available, may change the magnitude of the response of particular reefs to sea-level rise, the coarse-grained geographic patterns that emerged from the model projections were consistent through the various scenarios and model refinements and therefore have less uncertainty.

Indo-Pacific coral reefs that were predicted to be able to keep pace with sea-level rise by 2100 were in: 1) the Maldives, 2) the Chagos Archipelago, 3) northern Indonesia, 4) Micronesia, 5) the Marshall Islands, 6) the Solomon Islands, 7) Vanuatu and 8) Fiji (Fig. 5). Some reefs that were only marginally able to keep up with sea-level rise were predicted in the Seychelles, French Polynesia and northeastern Australia (Fig. 5, Supplementary material Appendix 1 Fig. A8). Protecting these marginal reefs from local disturbances such as local pollution and fishing pressure may increase their resilience and reef-building capacity. Furthermore, the models estimated that protecting reefs from overfishing should positively influence their rates of carbonate production.

Indeed, which reefs will keep up with sea-level rise is critically dependent on the drastic reduction of $\rm CO_2$ and other greenhouse gas emissions, and the reduction of local stressors including pollution and overfishing. Most troubling is the estimated 1 600 000 km² of reef habitat that are projected to be unable to produce enough carbonate to keep up with rising sea-level under the RCP 8.5 Wm² climate-change scenario (Table 3). However, the difference between RCPs 8.5 and 4.5 Wm² could mean the difference between < 5% and > 15% of Indo-Pacific coral reefs keeping up with sea-level rise by the year 2100, with the capacity to reach much higher rates of 21–27% (~350 000–470 000 km²) if rigorous reef

management reduces the burdens of local pollution and fishing pressure (Table 2).

Data availability statement

All R-code and SDM outputs are available at GitHub source: https://github.com/InstituteForGlobalEcology, Google Earth (.kml) files of raster outputs for carbonate production, net accretion in relation to sea-level rise, erosional and sedimentary forces, and predicted 2100 sea-level are also available at the GitHub source.

Acknowledgements – We would like to thank Sandra van Woesik for editorial suggestions that improved the manuscript. This is contribution number 216 from the Inst. of Global Ecology at the Florida Inst. of Technology.

Funding – We would like to thank the National Science Foundation (OCE 1657633 and OCE 1829393) for supporting our research.

References

- Ayre, D. J. and Hughes, T. P. 2000. Genotypic diversity and gene flow in brooding and spawning corals along the Great Barrier Reef, Australia. – Evolution 54: 1590–1605.
- Cacciapaglia, C. W. and van Woesik, R. 2015. Reef-coral refugia in a rapidly changing ocean. – Global Change Biol. 21: 2272–2282.
- Cacciapaglia, C. W. and van Woesik, R. 2016. Climate-change refugia: shading reef corals by turbidity. Global Change Biol. 22: 1145–1154.
- Carreiro-Silva, M. and McClanahan, T. R. 2001. Echinoid bioerosion and herbivory on Kenyan coral reefs: the role of protection from fishing. J. Exp. Mar. Biol. Ecol. 262: 133–153.
- Doney, S. C. et al. 2009. Ocean acidification: the other CO₂ problem. Annu. Rev. Mar. Sci. 1: 169–192.
- Edinger, E. N. and Risk, M. J. 1994. Oligocene–Miocene extinction and geographic restriction of Caribbean corals: roles of turbidity, temperature and nutrients. Palaios 9: 576–598.
- Edinger, E. N. et al. 2000. Normal coral growth rates on dying reefs: are coral growth rates good indicators of reef health?

 Mar. Pollut. Bull. 40: 404–425.
- Figueiredo, J. et al. 2014. Increased local retention of reef coral larvae as a result of ocean warming. Nat. Clim. Change 4: 498–502.
- Gouezo, M. et al. 2015. Impact of two sequential super typhoons on coral reef communities in Palau. Mar. Ecol. Prog. Ser. 540: 73–85.
- Hallock, P. and Schlager, W. 1986. Nutrient excess and the demise of coral reefs and carbonate platforms. Palaios 1: 389–398.
- Hijmans, R. et al. 2014. dismo: species distribution modeling.
 R package ver. 0.9-3, http://CRAN.R-project.org/package=dismo.
- Hoegh-Guldberg, O. et al. 2007. Coral reefs under rapid climate change and ocean acidification. Science 318: 1737–1742.
- Hubbard, D. K. 1986. Sedimentation as a control of reef development: St. Croix, USVI. Coral Reefs 5: 117–125.
- IPCC 2013. Climate change 2013: the physical science basis. Contribution of Working Group I to the Fifth Assessment Report of the Intergovernmental Panel on Climate Change. Cambridge Univ. Press.

- Jevrejeva, S. et al. 2014. Upper limit for sea level projections by 2100. Environ. Res. Lett. 9: 104008.
- Kleypas, J. A. 1997. Modeled estimates of global reef habitat and carbonate production since the last glacial maximum. Paleoceanography 12: 533–545.
- Kleypas, J. A. et al. 1999. Environmental limits to coral reef development: where do we draw the line? Am. Zool. 39: 146–159.
- Knutson, T. R. et al. 2010. Tropical cyclones and climate change.
 Nat. Geosci. 3: 157–163.
- Lambeck, K. and Chappell, J. 2001. Sea level change through the last glacial cycle. Science 292: 679–686.
- Loya, Y. et al. 2001. Coral bleaching: the winners and the losers. Ecol. Lett. 4: 122–131.
- Manzello, D. P. et al. 2012. Ocean acidification refugia of the Florida Reef tract. PLoS One 7: e41715.
- McClanahan, T. R. and Shafir, S. H. 1990. Causes and consequences of sea urchin abundance and diversity in Kenyan coral reef lagoons. Oecologia 83: 362–370.
- McCulloch, M. et al. 2012. Coral resilience to ocean acidification and global warming through pH up-regulation. Nat. Clim. Change 2: 623–627.
- Miller, K. and Mundy, C. 2003. Rapid settlement in broadcast spawning corals: implications for larval dispersal. Coral Reefs 22: 99–106.
- Moyer, A. C. et al. 2007. Comparison of observed gale radius statistics. Meteorol. Atmos. Phys. 97: 41–55.
- Muir, P. R. et al. 2015. Limited scope for latitudinal extension of reef corals. Science 348: 1135–1138.
- O'Connor, M. I. et al. 2007. Temperature control of larval dispersal and the implications for marine ecology, evolution and conservation. Proc. Natl Acad. Sci. USA 104: 1266–1271.
- Pari, N. et al. 1998. Bioerosion of experimental substrates on high islands and on atoll lagoons (French Polynesia) after two years of exposure. Mar. Ecol. Prog. Ser. 166: 119–130.
- Penn, J. L. et al. 2018. Temperature-dependent hypoxia explains biogeography and severity of end-Permian marine mass extinction. Science 362: eaat1327.
- Perry, C. T. et al. 2008. Carbonate budgets and reef production states: a geomorphic perspective on the ecological phase-shift concept. – Coral Reefs 27: 853–866.
- Perry, C. T. et al. 2013. Caribbean-wide decline in carbonate production threatens coral reef growth. Nat. Commun. 4: ncomms2409.
- Perry, C. T. et al. 2015. Remote coral reefs can sustain high growth potential and may match future sea-level trends. Sci. Rep. 5: 18289.
- Perry, C. T. et al. 2018. Loss of coral reef growth capacity to track future increases in sea level. Nature 558: 396–400.
- Pierson, D. C. et al. 2008. Relationship between the attenuation of downwelling irradiance at 490 nm with the attenuation of PAR (400 nm–700 nm) in the Baltic Sea. Remote Sens. Environ. 112: 668–680.
- Risk, M. J. et al. 2009. The use of δ15N in assessing sewage stress on coral reefs. Mar. Pollut. Bull. 58: 793–802.
- Rogers, C. S. 1990. Responses of coral reefs and reef organisms to sedimentation. Mar. Ecol. Prog. Ser. 62: 185–202.
- Sanders, M. I. et al. 2014. Interdependency of tropical marine ecosystems in response to climate change. Nat. Clim. Change 4: 724–729.
- Shanks, A. L. et al. 2003. Propagule dispersal distance and the size and spacing of marine reserves. Ecol. Appl. 13: S159–S169.
- Sully, S. et al. 2019. A global analysis of coral bleaching over the past two decades. Nat. Commun. 10: 1264.

- Szmytkiewicz, A. and Zalewska, T. 2014. Sediment deposition and accumulation rates determined by sediment trap and 210 Pb isotope methods in the Outer Puck Bay (Baltic Sea). Oceanologia 56: 85–106.
- Tyberghein, L. et al. 2012. Bio-ORACLE: a global environmental dataset for marine species distribution modelling. Global Ecol. Biogeogr. 21: 272–281.
- van Woesik, R. 2010. Calm before the spawn: global coral spawning patterns are explained by regional wind fields. Proc. R. Soc. B 277: 715–722.
- van Woesik, R. 2013 Quantifying uncertainty and resilience on coral reefs using a Bayesian approach. Environ. Res. Lett. 8: 044051.
- van Woesik, R. and Cacciapaglia, C. W. 2018. Keeping up with sea-level rise: carbonate production rates in Palau and Yap, western Pacific Ocean. PLoS One 13: e0197077.
- van Woesik, R. and Cacciapaglia, C. W. 2019. Carbonate production of Micronesian reefs suppressed by thermal

Supplementary material (available online as Appendix ecog-04949 at <www.ecograhy.org/appendix/ecog-04949>). Appendix 1.

- anomalies and *Acanthaster* as sea-level rises. PLoS One 14: e0224887.
- van Woesik, R. et al. 1991. Impact of tropical cyclone 'Ivor' on the Great Barrier Reef, Australia. J. Coastal Res. 7: 551–557.
- van Woesik, K. et al. 2013. Effects of ocean acidification on the dissolution rates of reef-coral skeletons. PeerJ 1: e208.
- Vermeer, M. and Rahmstorf, S. 2009. Global sea level linked to global temperature. Proc. Natl Acad. Sci. USA 106: 21527–21532.
- Veron, J. E. N. 2000. Corals of the world. Australian Inst. of Marine Science, Townsville, Australia.
- Wallace, C. C. 1999. Staghorn corals of the world: a revision of the coral genus *Acropora*. CSIRO Publishing.
- Williams, I. D. et al. 2011. Differences in reef fish assemblages between populated and remote reefs spanning multiple archipelagos across the central and western Pacific. J. Mar. Biol. 2011: 826234.